On the Instability of an Axially Moving Elastic Plate

N. Banichuk [a], J. Jeronen [b,*],
P. Neittaanmäki [b] and T. Tuovinen [b]

[a] *Institute for Problems in Mechanics RAS, prosp. Vernadskogo 101, block 1, Moscow 119526, Russian Federation*

[b] *Department of Mathematical Information Technology, Mattilanniemi 2 (Agora), 40014 University of Jyväskylä, Finland*

Abstract

Problems of stability of an axially moving elastic band travelling at constant velocity between two supports and experiencing small transverse vibrations are considered in a 2-D formulation. The model of a thin elastic plate subjected to bending and tension is used to describe the bending moment and the distribution of membrane forces. The stability of the plate is investigated with the help of an analytical approach. In the frame of a general dynamic analysis, it is shown that the onset of instability takes place in the form of divergence (buckling). Then the static forms of instability are investigated, and critical regimes are studied as functions of geometric and mechanical problem parameters. It is shown that in the limit of a narrow strip, the 2-D formulation reduces to the classical 1-D model. In the limit of a wide band, there is a small but finite discrepancy between the results given by the 1-D model and the full 2-D formulation, where the discrepancy depends on the Poisson ratio of the material. Finally, the results are illustrated via numerical examples, and it is observed that the transverse displacement becomes localised in the vicinity of free boundaries.

Key words: axially, moving, thin, plate, elastic, instability, analytical solutions

* Corresponding author. Tel.: +358 40 760 7328; fax: +358 14 260 2771.
Email address: juha.jeronen@jyu.fi (J. Jeronen).

1 Introduction

Travelling flexible strings, membranes, beams and plates are the most common models of axially moving materials. These models are frequently used for describing the mechanical behaviour of moving paper webs, magnetic tapes, films, transmission cables, swimming fish, and the like (Ulsoy et al. 1978, Lighthill 1960). In many applications the models of axially moving materials can be used for evaluation of a critical transport velocity that leads to the loss of stability. This is important because the occurrence of instability can cause, in particular, damage in a paper web and breakage of transmission cables.

Previous studies of these models, described by second and fourth-order differential equations, focus on the aspect of free vibrations including the nature of wave propagation in moving media and the effects of axial motion on the frequency spectrum and eigenfunctions. Investigations of the vibrations of travelling membranes and thin plates were first performed in Archibald and Emslie (1958), Miranker (1960), Swope and Ames (1963), Mote (1968), Mote (1972), Simpson (1973), Mote (1975), Ulsoy and Mote (1980), Mote and Ulsoy (1982), Chonan (1986), Wickert and Mote (1990) and Lin and Mote (1995). These studies were mainly devoted to various aspects of free vibration and forced vibrations.

Stability considerations were reviewed in Mote (1972). The effects of axial motion on the frequency spectrum and eigenfunctions were investigated in Archibald and Emslie (1958) and Simpson (1973). It was shown that the natural frequency of each mode decreases when transport speed increases, and that the travelling string and beam both experience divergence instability at a sufficiently high speed. Response prediction has been made for particular cases when excitation assumes special forms such as a constant transverse point force (Chonan 1986) or harmonic support motion (Miranker 1960). Arbitrary excitation and initial conditions have been analysed with the help of modal analysis and a Green function method in Wickert and Mote (1990). As a result, the associated critical speeds have been determined explicitly.

Lin and Mote (1996) predicted the wrinkling instability and the corresponding wrinkled shape of a web with small flexural stiffness. The stability and the vibration characteristics of an axially moving plate have been investigated by Lin (1997). The loss of stability was studied with application of dynamic and static approaches, and Wickert's (1992) approach to derive the equation of motion for the plate in matrix form and to use the Galerkin method. It was shown by means of numerical analysis that, for all cases dynamic instability (flutter) is realised when the frequency is zero and the critical velocity coincides with the corresponding velocity obtained from static analysis. In Shin et al. (2005), the out-of-plane vibration of an axially moving membrane was studied. Also here, it was found by numerical analysis,

that for a membrane with a no-friction boundary condition in the lateral direction along the rollers, the membrane remains dynamically stable until the critical speed, at which statical instability occurs.

This paper is devoted to application of analytical methods to instability analysis of an axially moving rectangular plate and to investigation of the dependence of the solution on the problem parameters. In the frame of the general dynamic approach, a functional expression for the characteristic index of stability is found and can be effectively used for frequency evaluation. It is shown analytically, that the loss of stability is realised for some critical velocity in a divergence mode, i.e. $V_0^{\mathrm{div}} < V_0^{\mathrm{fl}}$. Then a static analysis of instability is performed and the possible buckled forms of the plate (symmetric and antisymmetric) are studied as functions of geometric and mechanical problem parameters. In particular, we show that the buckled plate shape is symmetric and that the elastic deflections are localised in the vicinity of free edges of the plate. This localisation phenomenon is familiar from the eigenfunctions of stationary plates under in-plane compressive load (see e.g. Gorman 1982), and it can also be seen in the numerical results of Shin et al. (2005) for an axially travelling membrane.

It should be noted that when applied to the particular context of paper production, the present study ignores several potentially important effects. First of all, for a rigorous analysis, the orthotropic nature of paper should be accounted for. Secondly, the viscoelasticity, which introduces damping into the system, is ignored. This is not a major problem, as the introduction of damping is not expected to change the critical velocity, although it does modify the postdivergence behaviour (Mote and Ulsoy 1982). Finally, the interaction between the travelling web and the surrounding air, which is not accounted for in the present study, is known to influence the critical velocity (Pramila 1986, Frondelius et al. 2006) and the dynamical response (Kulachenko et al. 2007), possibly also affecting the buckling shape.

2 Basic relations for transverse vibrations of axially moving elastic plate

Let us investigate the elastic stability of a band travelling with a constant velocity V_0 in the x direction between two rollers located at $x = 0$ and $x = \ell$. Consider, in a cartesian coordinate system, a rectangular part of the band

$$\Omega : \ 0 \leq x \leq \ell, \ -b \leq y \leq b \ ,$$

where ℓ and b are prescribed parameters (Figure 1). Additionally assume that the considered part of the band is represented as a rectangular elastic plate having constant thickness h, Poisson ratio ν, Young modulus E, and bending rigidity D. The plate is subjected to homogeneous tension, T_0, acting in the x direction. The sides of the plate $x = 0$, $-b \leq y \leq b$ and $x = \ell$,

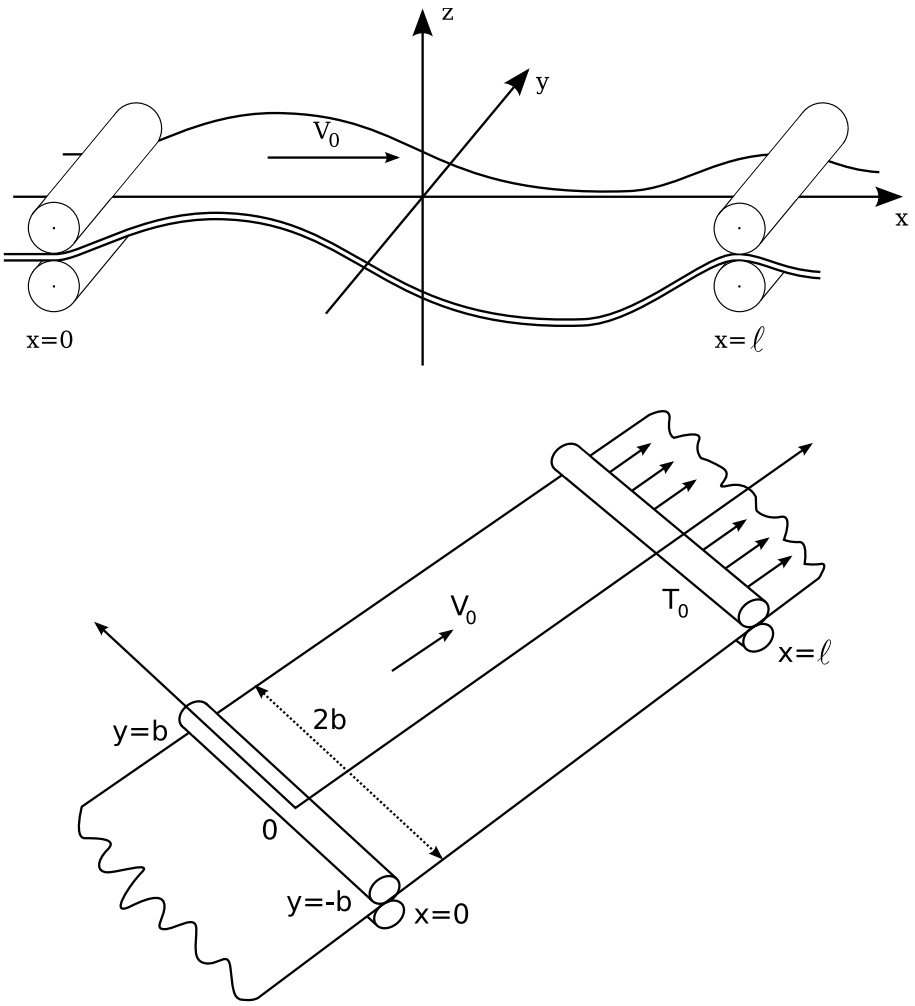

Figure 1. Axially moving elastic plate, simply supported at $x = 0$ and $x = \ell$.

$-b \leq y \leq b$ are simply supported and the sides $y = -b$, $0 \leq x \leq \ell$ and $y = b$, $0 \leq x \leq \ell$ are free of tractions.

The transverse displacement of the travelling band is described by the deflection function w which depends on the space coordinates $x,\ y$ and time t. The differential equation for small transverse vibrations has the form

$$m\frac{\mathrm{d}^2 w}{\mathrm{d}t^2} = T_{xx}\frac{\partial^2 w}{\partial x^2} + 2T_{xy}\frac{\partial^2 w}{\partial x \partial y} + T_{yy}\frac{\partial^2 w}{\partial y^2} - D\Delta^2 w \tag{1}$$

Here m is the mass per unit area of the middle surface of the plate, Δ^2 is the biharmonic operator, T_{xx}, T_{xy}, T_{yy} are in-plane tensions and

$$D\Delta^2 w = D\left(\frac{\partial^4 w}{\partial x^4} + 2\frac{\partial^2 w}{\partial x^2 \partial y^2} + \frac{\partial^4 w}{\partial y^4}\right), \quad D = \frac{Eh^3}{12(1-\nu^2)} \tag{2}$$

The total acceleration $\frac{\mathrm{d}^2 w}{\mathrm{d}t^2}$ on the left-hand side of the equation (1) is expressed as

$$\frac{\mathrm{d}^2 w}{\mathrm{d}t^2} = \frac{\mathrm{d}}{\mathrm{d}t}\left(\frac{\partial w}{\partial t} + V_0 \frac{\partial w}{\partial x}\right) = \frac{\partial^2 w}{\partial t^2} + 2V_0 \frac{\partial^2 w}{\partial x \partial t} + V_0^2 \frac{\partial^2 w}{\partial x^2}\,, \tag{3}$$

where the right-hand side in (3) contains three terms, representing respectively a local acceleration, a Coriolis acceleration and a centripetal acceleration. The in-plane tensions T_{xx}, T_{xy} and T_{yy} are assumed to satisfy the equilibrium equations

$$\frac{\partial T_{xx}}{\partial x} + \frac{\partial T_{xy}}{\partial y} = 0, \quad \frac{\partial T_{xy}}{\partial x} + \frac{\partial T_{yy}}{\partial y} = 0 \tag{4}$$

with the boundary conditions

$$T_{xx} = T_0, \quad T_{xy} = 0 \quad \text{at } x = 0,\ |y| \le b \text{ and } x = \ell,\ |y| \le b\,,$$

$$T_{yy} = 0, \quad T_{xy} = 0 \quad \text{at } y = \pm b, \quad 0 \le x \le \ell\,. \tag{5}$$

We assume that the deflection function w and its partial derivatives are small, and that they satisfy the boundary conditions corresponding to simply supported boundaries at $x = 0$, $|y| \le b$, and $x = \ell$, $|y| \le b$, and free boundaries at $|y| = b$, $0 \le x \le \ell$. That is (see, for example, Timoshenko and Woinowsky-Krieger 1959),

$$(w)_{x=0,\,\ell} = 0, \quad \left(\frac{\partial^2 w}{\partial x^2}\right)_{x=0,\,\ell} = 0\,, \quad -b \le y \le b \tag{6}$$

$$\left(\frac{\partial^2 w}{\partial y^2} + \nu \frac{\partial^2 w}{\partial x^2}\right)_{y=\pm b} = 0\,, \quad 0 \le x \le \ell \tag{7}$$

$$\left(\frac{\partial^3 w}{\partial y^3} + (2-\nu) \frac{\partial^3 w}{\partial x^2 \partial y}\right)_{y=\pm b} = 0\,, \quad 0 \le x \le \ell\,. \tag{8}$$

In the following we use stationary relations, i.e. it is supposed that $w = w(x, y)$ and all partial derivatives with respect to t are equal to zero. The following expressions for in-plane forces are found using the boundary conditions (5) and the partial differential equations (4):

$$T_{xx}(x, y) = T_0, \quad T_{yy}(x, y) = T_{xy}(x, y) = 0 \quad (x, y) \in \Omega\,. \tag{9}$$

Thus, we have the following dynamic equation for small vibrations of the

travelling plate:

$$\mathfrak{L}(w) = \frac{\partial^2 w}{\partial t^2} + 2V_0\frac{\partial^2 w}{\partial x \partial t} + (V_0^2 - C^2)\frac{\partial^2 w}{\partial x^2} + \frac{D}{m}\left(\frac{\partial^4 w}{\partial x^4} + 2\frac{\partial^2 w}{\partial x^2 \partial y^2} + \frac{\partial^4 w}{\partial y^4}\right) = 0\,, \quad C = \sqrt{\frac{T_0}{m}}\,. \tag{10}$$

As is seen from (6)-(10), our boundary-value problem is homogeneous and invariant with respect to the symmetry operation $y \to -y$, and consequently, all solutions of the problem can be considered as symmetric or antisymmetric functions of y, i.e.,

$$w(x,y,t) = w(x,-y,t) \quad \text{or} \quad w(x,y,t) = -w(x,-y,t)\,. \tag{11}$$

3 Dynamic behaviour of transverse vibrations and divergence mode of elastic instability

Let us represent the solution of our dynamic boundary-value problem as (Bolotin 1963)

$$w(x,y,t) = W(x,y)e^{i\omega t}\,, \tag{12}$$

or in the equivalent form

$$w(x,y,t) = W(x,y)e^{st}\,, \tag{13}$$

where ω is the frequency of small transverse vibrations and

$$s = i\omega \tag{14}$$

is the complex characteristic parameter:

$$s = \mathrm{Re}\; s + i\;\mathrm{Im}\; s = s_{\mathrm{re}} + i\; s_{\mathrm{im}} \tag{15}$$

If this parameter is pure imaginary, i.e.,

$$\mathrm{Re}\; s = 0, \quad \mathrm{Im}\; s \neq 0, \tag{16}$$

and consequently ω is a real value, the plate performs harmonic vibrations of small amplitude and its motion can be considered stable. If, for some values of the problem parameters, the real part of the characteristic index becomes positive, i.e.,

$$s_{\mathrm{re}} = \mathrm{Re}\; s > 0, \tag{17}$$

the transverse vibrations grow exponentially and consequently the behaviour of the plate is unstable. To investigate the dynamic behaviour of the plate,

we insert the representation (13) into equation (10). We have

$$s^2 W + 2sV_0 \frac{\partial W}{\partial x} + (V_0^2 - C^2)\frac{\partial^2 W}{\partial x^2} + \frac{D}{m}\Delta^2 W = 0. \tag{18}$$

We multiply the left-hand side of equation (18) by W and perform integration over the domain Ω to obtain

$$s^2 \int_\Omega W^2 \, \mathrm{d}\Omega + 2sV_0 \int_\Omega W \frac{\partial W}{\partial x} \, \mathrm{d}\Omega + (V_0^2 - C^2) \int_\Omega W \frac{\partial^2 W}{\partial x^2} \, \mathrm{d}\Omega + \frac{D}{m} \int_\Omega W \Delta^2 W \, \mathrm{d}\Omega = 0 \, . \tag{19}$$

Because

$$\begin{aligned} \int_\Omega W \frac{\partial W}{\partial x} \, \mathrm{d}\Omega &= \int_{-b}^{b} \int_0^\ell W \frac{\partial W}{\partial x} \, \mathrm{d}x \, \mathrm{d}y \\ &= \int_{-b}^{b} \left[\frac{W^2(\ell, y)}{2} - \frac{W^2(0, y)}{2} \right] \mathrm{d}y \, , \end{aligned}$$

we find by by applying the boundary conditions (6) that

$$\int_\Omega W \frac{\partial W}{\partial x} \, \mathrm{d}\Omega = 0 \, . \tag{20}$$

In a similar manner, by performing integration by parts and again applying the boundary conditions (6), we have

$$\int_\Omega W \frac{\partial^2 W}{\partial x^2} \, \mathrm{d}\Omega = - \int_\Omega \left(\frac{\partial W}{\partial x} \right)^2 \mathrm{d}\Omega \, . \tag{21}$$

The last integral in (19) can be estimated, by using Green's 2nd identity, as

$$\int_\Omega W \Delta^2 W \, \mathrm{d}\Omega = \int_\Omega (\Delta W)^2 \, \mathrm{d}\Omega + \int_\Gamma \left(W \frac{\partial}{\partial n} \Delta W - \Delta W \frac{\partial W}{\partial n} \right) \mathrm{d}\Gamma, \tag{22}$$

where n is the outside unit normal to the boundary. In order to evaluate the contour integral in (22) we divide the boundary Γ into four parts (see Figure 2):

$$\Gamma_-(0 \le x \le \ell, \; y = -b), \qquad \Gamma_r(x = \ell, \; -b \le y \le b),$$

$$\Gamma_+(0 \le x \le \ell, \; y = b), \qquad \Gamma_\ell(x = 0, \; -b \le y \le b).$$

Admitting counterclockwise integration along Γ, we have

$$I = \int_\Gamma \left(W \frac{\partial}{\partial n} \Delta W - \Delta W \frac{\partial W}{\partial n} \right) \mathrm{d}\Gamma = I_- + I_r + I_+ + I_\ell. \tag{23}$$

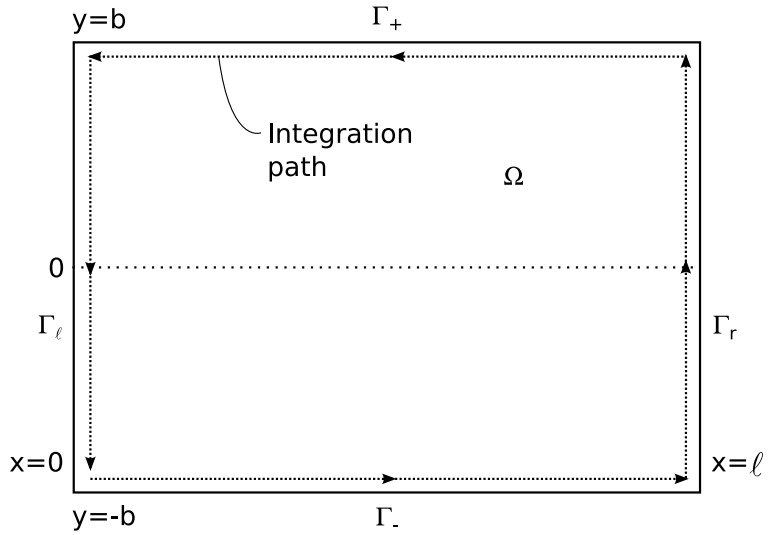

Figure 2. Division of the boundary Γ for the investigated contour integral .

Here

$$I_i = \int_{\Gamma_i} \left(W \frac{\partial}{\partial n} \Delta W - \Delta W \frac{\partial W}{\partial n} \right) \mathrm{d}\Gamma = 0, \quad i = r, \ell \tag{24}$$

$$\begin{aligned} I_- &= \int_{\Gamma_-} \left(W \frac{\partial}{\partial n} \Delta W - \Delta W \frac{\partial W}{\partial n} \right) \mathrm{d}\Gamma \\ &= - \int_0^\ell \left(W \frac{\partial}{\partial y} \Delta W - \Delta W \frac{\partial W}{\partial y} \right)_{y=-b} \mathrm{d}\Gamma \end{aligned} \tag{25}$$

$$\begin{aligned} I_+ &= \int_{\Gamma_+} \left(W \frac{\partial}{\partial n} \Delta W - \Delta W \frac{\partial W}{\partial n} \right) \mathrm{d}\Gamma \\ &= - \int_0^\ell \left(W \frac{\partial}{\partial y} \Delta W - \Delta W \frac{\partial W}{\partial y} \right)_{y=b} \mathrm{d}\Gamma \, . \end{aligned} \tag{26}$$

To transform (24)-(26) we have used the relations

$$\begin{gathered} \mathrm{d}\Gamma = \mathrm{d}x, \quad \frac{\partial}{\partial n} = -\frac{\partial}{\partial y} \quad \text{for } (x,y) \ \in \Gamma_- \, , \\ \mathrm{d}\Gamma = -\mathrm{d}x, \quad \frac{\partial}{\partial n} = \frac{\partial}{\partial y} \quad \text{for } (x,y) \ \in \Gamma_+ \, , \\ W = \Delta W = 0 \quad \text{for } (x,y) \ \in \Gamma_\ell + \Gamma_r \, . \end{gathered} \tag{27}$$

Thus, we have

$$I = I_- + I_+ = - \int_0^\ell (Q_{y=b} + Q_{y=-b}) \mathrm{d}x \, , \tag{28}$$

where

$$Q = W\frac{\partial}{\partial y}\Delta W - \Delta W\frac{\partial W}{\partial y}\,. \tag{29}$$

Using the boundary conditions (7) and (8), we perform the transformations

$$(\Delta W)_{y=\pm b} = \left(\frac{\partial^2 W}{\partial x^2} + \frac{\partial^2 W}{\partial y^2}\right)_{y=\pm b} = (1-\nu^{-1})\left(\frac{\partial^2 W}{\partial y^2}\right)_{y=\pm b} \tag{30}$$

$$\left(\frac{\partial \Delta W}{\partial y}\right)_{y=\pm b} = \left(\frac{\partial^2 W}{\partial x^2 \partial y} + \frac{\partial^3 W}{\partial y^3}\right)_{y=\pm b} = \frac{1-\nu}{2-\nu}\left(\frac{\partial^3 W}{\partial y^3}\right)_{y=\pm b}\,,$$

and find

$$Q = (1-\nu)\left(\frac{1}{2-\nu}W\frac{\partial^3 W}{\partial y^3} + \frac{1}{\nu}\frac{\partial W}{\partial y}\frac{\partial^2 W}{\partial y^2}\right). \tag{31}$$

We can see from (11) and (31) that the function Q is antisymmetric with respect to the transformation $y \to -y$ (for both symmetric and antisymmetric functions W), and consequently,

$$Q_{y=b} + Q_{y=-b} = 0, \quad \Rightarrow \quad I = 0. \tag{32}$$

Thus the boundary term in (22) vanishes and we obtain

$$\int_\Omega W\Delta^2 W \,\mathrm{d}\Omega = \int_\Omega (\Delta W)^2 \,\mathrm{d}\Omega\,. \tag{33}$$

It follows from (19)-(21) and (33) that

$$\omega^2 = -s^2 = \frac{(C^2 - V_0^2)\displaystyle\int_\Omega \left(\frac{\partial W}{\partial x}\right)^2 \mathrm{d}\Omega + \frac{D}{m}\int_\Omega (\Delta W)^2 \,\mathrm{d}\Omega}{\displaystyle\int_\Omega W^2 \,\mathrm{d}\Omega}\,. \tag{34}$$

All the integrals in (34) are positive. We see that s^2 is initially ($V_0 = 0$) negative, meaning s is purely imaginary, which corresponds to a mode with stable harmonic oscillation. As V_0 is increased, the first term in the numerator vanishes when $V_0 = C$. Upon further increase of V_0, the first term becomes negative, and at some point (depending on the bending rigidity D) it will balance out the second term and s becomes zero. At this point we have the steady-state solution (buckling) at some velocity $V_0 = V_0^{\mathrm{div}}$ (Figure 3). At this moment, as is seen from (34), the following relation between the critical velocity and the divergent mode holds:

$$\left(V_0^{\mathrm{div}}\right)^2 = C^2 + \frac{D}{m}\frac{\displaystyle\int_\Omega (\Delta W)^2 \mathrm{d}\Omega}{\displaystyle\int_\Omega \left(\frac{\partial W}{\partial x}\right)^2 \mathrm{d}\Omega}\,. \tag{35}$$

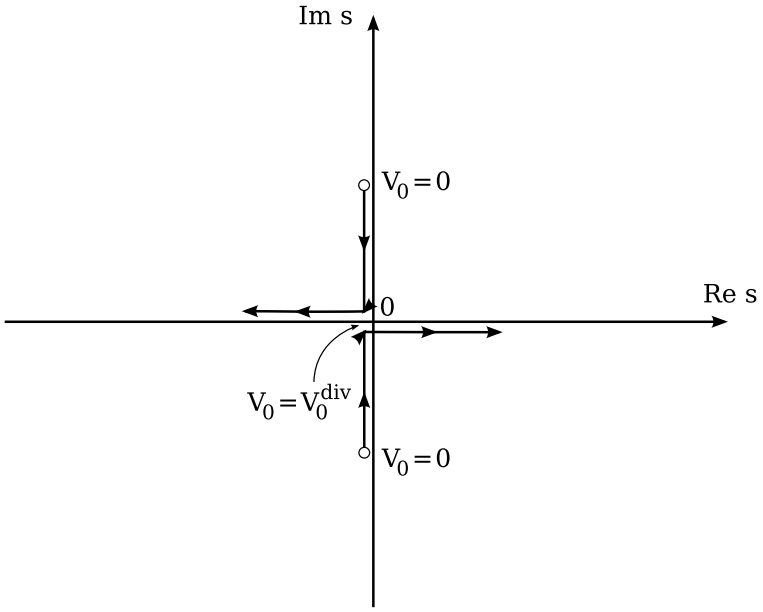

Figure 3. Behaviour of the characteristic exponent s.

In particular, it is follows from (35) that when bending rigidity of the band is negligibly small, then $\left(V_0^{\text{div}}\right)^2 = C^2$.

If V_0 is still further increased, s becomes purely real, and the displacement of the plate grows exponentially with time.

Note that s will always pass through the origin before its real part becomes nonzero. Therefore, the problem setup of a simply supported axially moving elastic plate with free edges always exhibits statical instability first, and flutter modes are not realised.

4 Static analysis of stability loss

Taking into account the result (34), we may limit our consideration to a statical analysis. The stability problem considered in the frame of stationary equations is known as a buckling problem. This problem is formulated as the eigenvalue problem for the partial differential equation

$$(mV_0^2 - T_0)\frac{\partial^2 w}{\partial x^2} + D\left(\frac{\partial^4 w}{\partial x^4} + 2\frac{\partial^2 w}{\partial x^2 \partial y^2} + \frac{\partial^4 w}{\partial y^4}\right) = 0, \tag{36}$$

with the boundary conditions (6)-(8). To determine the minimal eigenvalue

$$\lambda = \gamma^2 = \frac{\ell^2}{\pi^2 D}(mV_0^2 - T_0) \tag{37}$$

of the problem (6)-(8), (36), and the corresponding eigenfunction $w = w(x, y)$, known as the divergence or buckling form, we apply the following representation:

$$w = w(x, y) = f\left(\frac{\pi y}{\ell}\right) \sin\left(\frac{\pi x}{\ell}\right), \tag{38}$$

where $f(\frac{\pi y}{\ell})$ is an unknown function. It follows from (38), that the desired buckling form w satisfies the boundary condition (6). Using dimensionless variables

$$\eta = \frac{\pi y}{\ell}, \quad \mu = \frac{\ell}{\pi b}, \tag{39}$$

and the relations (7)-(8), (36)-(39), we obtain the following eigenvalue problem for the unknown function $f(\eta)$:

$$\frac{\mathrm{d}^4 f}{\mathrm{d}\eta^4} - 2\frac{\mathrm{d}^2 f}{\mathrm{d}\eta^2} + (1-\lambda)f = 0, \quad -\frac{\pi b}{\ell} \le \eta \le \frac{\pi b}{\ell} \tag{40}$$

$$\frac{\mathrm{d}^2 f}{\mathrm{d}\eta^2} - \nu f = 0, \quad \eta = \pm\frac{\pi b}{\ell} \tag{41}$$

$$\frac{\mathrm{d}^3 f}{\mathrm{d}\eta^3} - (2-\nu)\frac{\mathrm{d}f}{\mathrm{d}\eta} = 0, \quad \eta = \pm\frac{\pi b}{\ell}\,. \tag{42}$$

The spectral boundary value problem (40)-(42) is invariant with respect to the symmetry operation $\eta \to -\eta$, and consequently, all its eigenfunctions (40)-(42) can be classified as

$$f^s(\eta) = f^s(-\eta), \quad f^a(\eta) = -f^a(-\eta), \quad 0 \le \eta \le \frac{\pi b}{\ell}\,. \tag{43}$$

Here f^s and f^a are, respectively, functions that are symmetric and antisymmetric (skew-symmetric) with respect to the x-axis.

When $\gamma \le 1$, a divergence mode which is symmetric with respect to the x-axis, can be presented in the form

$$w = f^s(\eta) \sin\left(\frac{\pi x}{\ell}\right) \tag{44}$$

$$f^s(\eta) = A^s \cosh(\kappa_+\eta) + B^s \cosh(\kappa_-\eta) \tag{45}$$

$$\kappa_+ = \sqrt{1+\gamma}\,, \quad \kappa_- = \sqrt{1-\gamma} \tag{46}$$

where $f^s(\eta)$ is a symmetric solution of (40), and A^s and B^s are arbitrary constants. We will return to the antisymmetric case at the end of section 4.

Using the relations (41)-(45), we can derive the linear algebraic equations for determining the constants A^s and B^s :

$$A^s(\kappa_+^2 - \nu) \cosh\left(\frac{\kappa_+}{\mu}\right) + B^s(\kappa_-^2 - \nu) \cosh\left(\frac{\kappa_-}{\mu}\right) = 0 \tag{47}$$

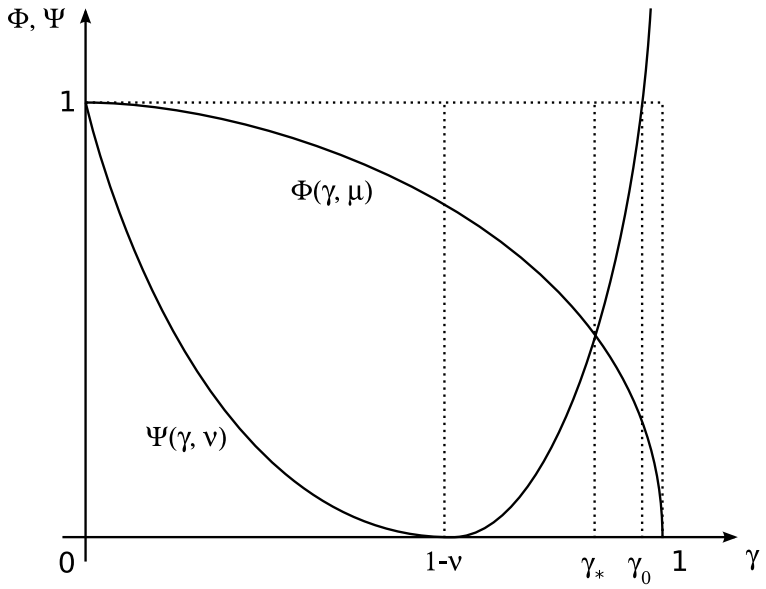

Figure 4. Behaviour of Φ and Ψ as functions of γ. Qualitative drawing.

$$-A^s\kappa_+(\kappa_-^2-\nu)\ \sinh\left(\frac{\kappa_+}{\mu}\right)-B^s\kappa_-(\kappa_+^2-\nu)\ \sinh\left(\frac{\kappa_-}{\mu}\right)=0\ .$$

The condition for a non-trivial solution to exist in the form (44)-(46) is that the determinant of the system (47) must vanish. This leads to the transcendental equation

$$\Delta^s(\gamma,\mu)=\kappa_-(\kappa_+^2-\nu)^2\ \cosh\left(\frac{\kappa_+}{\mu}\right)\ \sinh\left(\frac{\kappa_-}{\mu}\right)$$
$$-\kappa_+(\kappa_-^2-\nu)^2\ \sinh\left(\frac{\kappa_+}{\mu}\right)\ \cosh\left(\frac{\kappa_-}{\mu}\right)=0, \quad (48)$$

which determines the eigenvalues $\lambda=\gamma^2$ as an implicit function of the parameter $\mu=\frac{\ell}{\pi b}$. Equation (48) can be transformed into a more convenient form

$$\Phi(\gamma,\mu)-\Psi(\gamma,\nu)=0, \quad (49)$$

where

$$\Phi(\gamma,\mu)=\tanh\left(\frac{\sqrt{1-\gamma}}{\mu}\right)\ \coth\left(\frac{\sqrt{1+\gamma}}{\mu}\right),$$

$$\Psi(\gamma,\nu)=\frac{\sqrt{1+\gamma}}{\sqrt{1-\gamma}}\frac{(\gamma+\nu-1)^2}{(\gamma-\nu+1)^2}\ . \quad (50)$$

In the following we investigate the properties of the functions $\Phi(\gamma,\mu)$ and $\Psi(\gamma,\nu)$, expressed by (50), when $0\leq\gamma\leq 1$. See Figure 4.

As γ increases from zero to unity, the function $\Phi(\gamma,\mu)$ decreases continu-

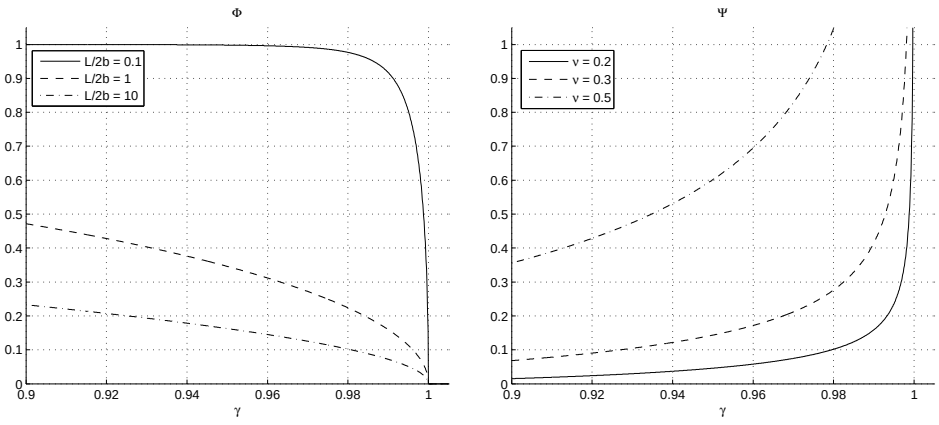

Figure 5. Plots of Φ (left) and Ψ (right) for different values of the parameters $\ell/2b$ and ν.

ously and monotonically from 1 to 0, i.e.

$$1 \geq \Phi(\gamma,\mu) \geq 0, \quad \frac{\partial\Phi(\gamma,\mu)}{\partial\gamma} < 0, \quad 0 \leq \gamma \leq 1 \tag{51}$$

$$\Phi(0,\mu) = \left(\tanh\frac{\sqrt{1-\gamma}}{\mu}\ \coth\frac{\sqrt{1+\gamma}}{\mu}\right)_{\gamma=0} = 1$$
$$\Phi(1,\mu) = \left(\tanh\frac{\sqrt{1-\gamma}}{\mu}\ \coth\frac{\sqrt{1+\gamma}}{\mu}\right)_{\gamma=1} = 0$$

The function $\Psi(\gamma,\nu)$ decreases from 1 to 0 in the interval $0 < \gamma < 1-\nu$,

$$1 \geq \Psi(\gamma,\nu) \geq 0, \quad \frac{\partial\Psi(\gamma,\nu)}{\partial\gamma} < 0, \quad 0 < \gamma < 1-\nu \tag{52}$$

$$\Psi(0,\nu) = \left[\frac{\sqrt{1+\gamma}}{\sqrt{1-\gamma}}\frac{(\gamma+\nu-1)^2}{(\gamma-\nu+1)^2}\right]_{\gamma=0} = 1$$
$$\Psi(1-\nu,\nu) = \left[\frac{\sqrt{1+\gamma}}{\sqrt{1-\gamma}}\frac{(\gamma+\nu-1)^2}{(\gamma-\nu+1)^2}\right]_{\gamma=1-\nu} = 0\,,$$

whereas it increases monotonically in the interval $1-\nu < \gamma < 1$ and takes values as large as are desired when $\gamma \to 1$,

$$0 \leq \Psi(\gamma,\nu) < \infty, \quad \frac{\partial\Psi(\gamma,\nu)}{\partial\gamma} > 0, \quad 1-\nu < \gamma < 1 \tag{53}$$

$$\Psi(1-\nu,\nu) = 0, \quad \lim_{\gamma\to 1}\Psi(\gamma,\nu) = \infty$$

Plots of the function $\Phi(\gamma,\mu)$ when $\frac{\ell}{2b} = 0.1,\ 1$ and 10 ($\mu = \frac{\ell}{\pi b}$) are shown in Figure 5 on the left. The functions $\Psi(\gamma,\nu)$ when $\nu = 0.2$, 0.3 and 0.5 are shown on the right.

The value of $\gamma = \gamma_0$ for which

$$\Psi(\gamma_0, \nu) = 1, \quad \gamma_0 \in [1-\nu, 1] \tag{54}$$

is of special interest. On solving the corresponding equation, we obtain

$$\gamma_0^2 = (1-\nu)(3\nu - 1 + 2\sqrt{1 - 2\nu(1-\nu)}) \tag{55}$$

The value of γ_0 turns out to be to close to unity. The values of $\lambda = \gamma_0^2$ are presented in Table 1 for different values of the Poisson ratio ν.

Assuming that $\ell \gg b$ (a long band span) so that $\mu = \frac{\ell}{\pi b}$ is large, we have the approximate expression

$$\Psi = \sqrt{\frac{1-\gamma}{1+\gamma}} \tag{56}$$

and the equation (49) admits the solution

$$\lambda_e = \gamma_e^2 = 1 - \nu^2 \, . \tag{57}$$

This solution corresponds to a narrow strip which is simply supported at its ends and leads to the Euler value of the force for stability loss (buckling)

$$P = P_e = \lambda_e \frac{\pi^2 D}{\ell^2} = \pi^2 \frac{EI}{\ell^2} \, , \tag{58}$$

where

$$P = mV_0^2 - T_0, \quad D = \frac{Eh^3}{12(1-\nu^2)}, \quad I = \frac{h^3}{12}. \tag{59}$$

Thus, we find that the case of a narrow strip corresponds to the classical one-dimensional case.

It follows from the above treatment and the properties of the functions $\Phi(\gamma, \mu)$ and $\Psi(\gamma, \nu)$, that the roots $\gamma = \gamma_*$ of the equation (49) lie in the interval

$$\gamma_e \leq \gamma_* \leq \gamma_0 \tag{60}$$

for all $0 < \mu < \infty$.

The corresponding critical velocity of the travelling band is represented as

$$(V_0)_*^2 = \frac{T_0}{m} + \frac{\gamma_*^2}{m} \left(\frac{\pi^2 D}{\ell^2} \right) \, . \tag{61}$$

In the limit of a wide band we have

$$\gamma_* \to \gamma_0 \neq 1 \quad \text{for } \mu = \frac{\ell}{\pi b} \to 0, \tag{62}$$

and therefore, the corresponding mode of stability loss (44)-(46) does not turn out to be cylindrical. Thus, the case of a wide band does not reduce to the classical one-dimensional case.

The largest difference between the critical parameter γ_*, which leads to the loss of stability of an infinitely wide band, and the corresponding value, obtained assuming a distribution of the deflections in the form of cylindrical surface, occurs when $\nu = 0.5$, i.e., in the case of an absolutely incompressible material.

Let us consider the possibility of modes of buckling which are antisymmetric about the x-axis:

$$w = f^a(\eta)\ \sin\left(\frac{\pi x}{\ell}\right)\ , \tag{63}$$

where

$$f^a(\eta) = A^a \sinh(\kappa_+\eta) + B^a \sinh(\kappa_-\eta) \tag{64}$$

for $\gamma \leq 1$. Here $\eta = \frac{\pi y}{\ell}$ and the values κ_+, κ_- are defined by the expressions (46). Using the expression (64) for f^a and the boundary conditions on the free edges of the plate (41)-(42), we obtain the following transcendental equation for determining the quantity γ:

$$\Phi(\gamma, \mu) - \Psi^{-1}(\gamma, \nu) = 0\ . \tag{65}$$

In (65), $\Phi(\gamma, \mu)$ and $\Psi(\gamma, \nu)$ are again defined by the formulas (50). In the segment $0 \leq \gamma \leq 1$ being considered, the equation has two roots,

$$\begin{gathered} \gamma = \gamma_1 \quad \rightarrow \quad \gamma_0 < \gamma_1 < 1 \quad \text{and} \\ \gamma = \gamma_2 \quad \rightarrow \quad \gamma_2 = 1, \end{gathered} \tag{66}$$

for arbitrary values of ν and the parameter μ, which characterizes the elongation of the plate.

Taking into account (60) and (66), we see that

$$\gamma_* < \gamma_1 < \gamma_2\ ,$$

so the minimal eigenvalue is γ_*. Thus, the critical buckling mode is symmetric with respect to the x-axis, and corresponds to $\gamma = \gamma_*$, i.e., the solution of equation (49).

5 Numerical results

In this section we present some numerical results. First, we describe the methods used, and show an example of the eigenvalues in one particular case (Figure 6). We then observe that the deflections are localised near the free edges (Figure 7), and investigate the sensitivity of this phenomenon on

the geometry and Poisson ratios of the plate (Figure 8). Finally, we evaluate the divergence speed for a selection of different geometry and Poisson ratios, with other physical parameters given and kept constant (Table 2).

Note that the dimensionless parameters ν and μ fully determine the localisation behaviour, as can be seen from equation (49), which implicitly defines the eigenvalue γ. The other physical parameters T_0, D and m have no effect on the localisation. The divergence velocity, on the other hand, depends on the values of all the physical parameters, but as the dependence is explicitly given by equation (61), we only evaluate one example case.

Based on the theory given in the sections above, the root $\gamma = \gamma_*$ of equation (49) was searched numerically in the interval $[0 + \varepsilon,\ 1 - \varepsilon]$, where the numerical parameter ε, used to avoid singularities, is small (10^{-8}). The critical value γ_0 was evaluated directly from the analytical expression (55), and the root corresponding to the antisymmetric case, $\gamma = \gamma_1$, was found numerically from (65) using $[\gamma_0 - \varepsilon,\ 1 - \varepsilon]$ as the search interval.

Once the eigenvalue γ_* of the symmetric case was found, the corresponding eigenfunction was constructed by inserting the eigenvalue into (46), (47). It is possible to eliminate either A^s or B^s from the first equation of the system (47). We chose to eliminate B^s; we have $B^s = -A^s \cdot (\kappa_+^2 - \nu)\ \cosh(\kappa_+/\mu) \cdot ((\kappa_-^2 - \nu)\ \cosh(\kappa_-/\mu))^{-1}$. Because multiplying by a constant does not affect the eigenfunction property, an arbitrary value may then be assigned to the constant A^s. We chose $A^s = 1$, and after evaluating $w^s(x, y)$ using this choice, normalised the final result by scaling the maximum value to unity. In case the denominator was zero, we set $A^s = 0$ and assigned $B^s = 1$.

For an incompressible material ($\nu = 0.5$), it was observed that the separation between the symmetric and antisymmetric eigenvalues was at its clearest when $\ell/2b \approx 1/5$. Figure 6 shows the left-hand sides of equations (49) and (65) as functions of γ, using these parameters. The eigenvalues, located at the zeros of the functions, are marked in the Figure.

In Figure 7, we can observe a localisation phenomenon: most of the displacement in the buckling mode occurs near the free edges. This phenomenon becomes more pronounced as the width of the plate grows with respect to its length. The compressibility of the material also affects the localisation phenomenon. The effect is at its strongest when $\nu = 0.5$, and it disappears completely in the limit $\nu \to 0$.

If $\ell/2b$ was increased from $1/5$, both the symmetric and antisymmetric solutions very rapidly converged to their respective limits. Already at $\ell/2b = 1/4$, the eigenvalue γ_1 was already so close to 1, that with the value of ε used, the function zero search was unable to detect it.

In the other limit, at $\ell/2b = 1/30$ the solutions converged to γ_0 such that the first six decimal places of γ_*, γ_0 and γ_1 were the same.

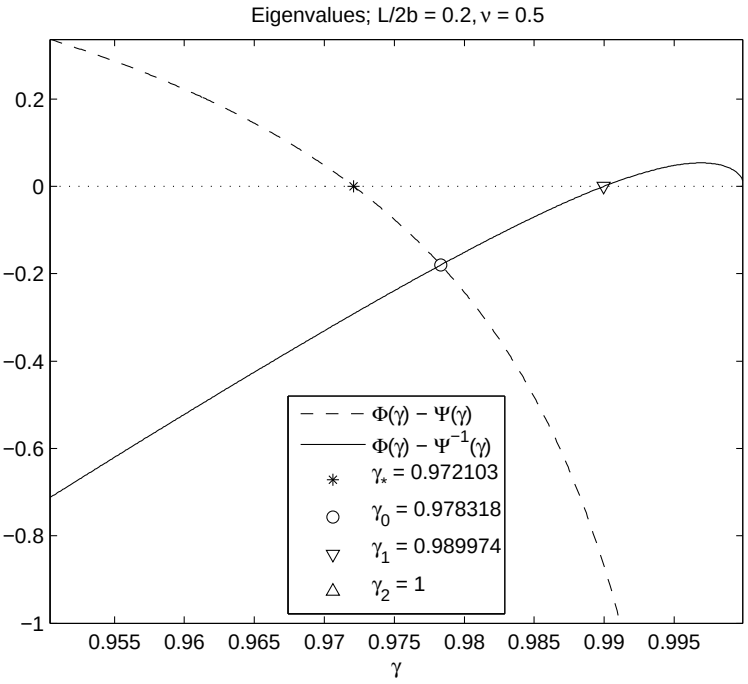

Figure 6. Eigenvalues of the symmetric (γ_*) and antisymmetric (γ_1, γ_2) modes for $\ell/2b = 1/5$, $\nu = 0.5$. The critical parameter γ_0 is the value of γ for which $\Psi(\gamma, \nu) = 1$.

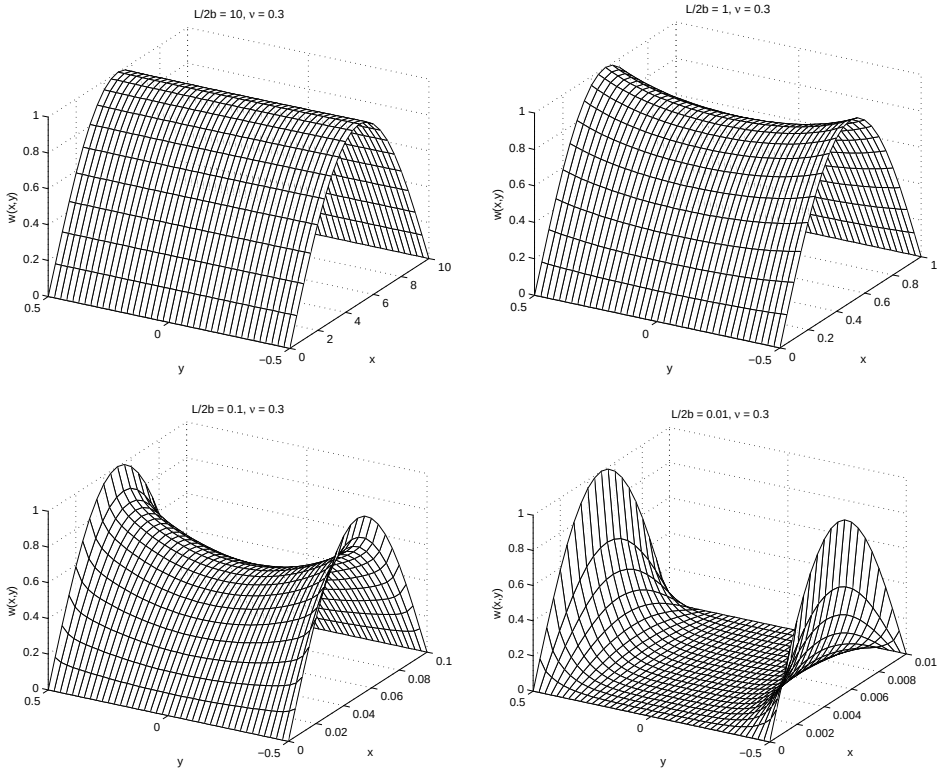

Figure 7. Localisation of deflections in the vicinity of the free boundaries.

In the limit of a perfectly compressible material ($\nu \to 0$) with $\ell/2b = 1/5$ kept constant, γ_*, γ_0 and γ_1 were observed to converge to unity. In this limit the buckling mode becomes cylindrical (no localisation).

Figure 8 represents the effect of the parameters $c \equiv \ell/2b$ and ν on the localisation phenomenon. The shade of each point of the figure indicates the degree of localisation of the corresponding eigenfunction. To obtain the degree of localisation for a given parameter pair (c, ν), we calculated the eigenfunction w, and then evaluated the localisation functional

$$L(\hat{w}) = \alpha \int_{-b}^{b} 1 - \hat{w}(\ell/2, y)\, \mathrm{d}y\,, \tag{67}$$

where

$$\hat{w}(x, y) = \Big| \frac{w(x, y)}{\max\limits_{(x,y)\in\Omega} |w(x, y)|} \Big| \tag{68}$$

and α is an arbitrary constant for normalisation.

The functional (67) was chosen, because w is of the form $w = f(y) \cdot g(x)$, and the x dependence is given by $\sin\left(\frac{\pi x}{\ell}\right)$. Thus, all the necessary information about the localisation effect is present in a single slice $w(x_0, y)$ for a constant x_0. The choice $x_0 = \ell/2$ is particularly convenient because $\sin(\pi/2) = 1$.

We see from (67) that if $\hat{w}(\ell/2, y) \equiv 1$, then $L(\hat{w}) = 0$, and for localised deflections of the type depicted in Figure 7, $L(\hat{w}) > 0$. In the limit case of $\hat{w}(\ell/2, y) \equiv 0$ (excepting the two points $y = \pm b$), we have $L(\hat{w}) = 2b\alpha$.

For the plot in Figure 8, we normalised the result by choosing α such that

$$\max_{(c,\nu)\in S} L(\hat{w}) = 1\,,$$

where $S = [c_{\min}, c_{\max}] \times [\nu_{\min}, \nu_{\max}]$, the chosen plot range for the problem parameters.

Finally, we evaluated the divergence speed V_0^{div} for some example cases. For the physical parameters in equation (61), where D is defined by equation (2), we used values typical for the papermaking process: $E = 10^9$ Pa, $h = 10^{-4}$ m, $m = 80$ g/m^2 and $T_0 = 500$ N/m. Note that as far as geometry is concerned, the divergence speed depends directly only on the length of the plate. Width, and thus, geometry ratio, dependence is introduced implicitly via the γ_*^2 term in (61).

The results of the divergence speed calculation are shown in Table 2. The row with $\nu = 0.3$ corresponds to the plots in Figure 7. We observe the conclusion indicated by the analysis in the previous section: the difference between the one-dimensional limit of $V_0^{\mathrm{div}} = \sqrt{T/m} \approx 79.0569$ m/s and the

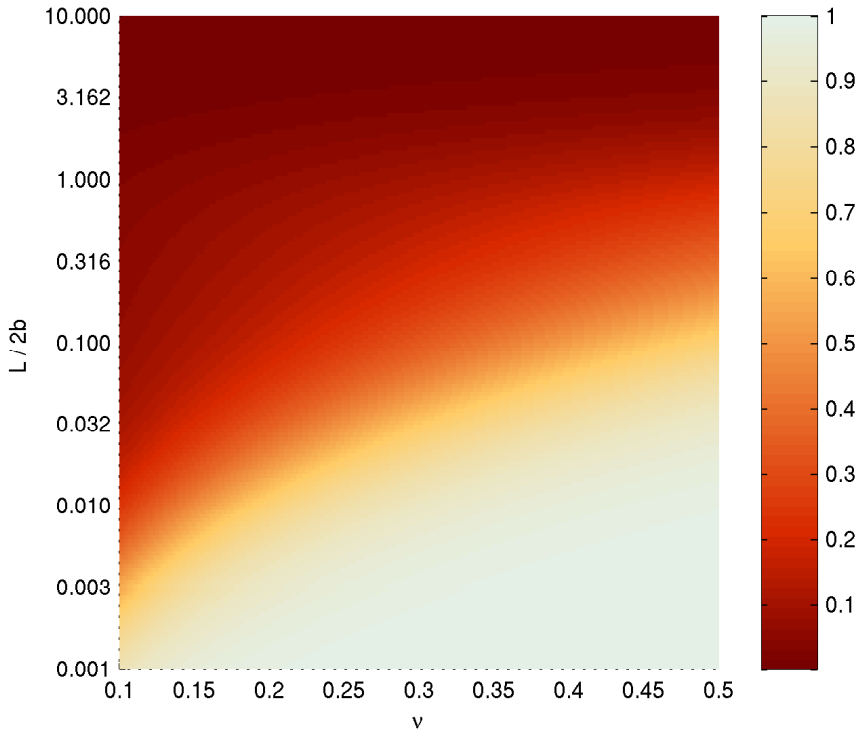

Figure 8. Relative strength of the localisation phenomenon as a function of the problem parameters. Note the logarithmic vertical axis.

divergence speed given by the two-dimensional model is the largest when the material is incompressible ($\nu = 0.5$) and the length to width ratio is small.

6 Conclusion

The loss of stability of axially moving plates was investigated in a two-dimensional formulation, taking into account their bending resistance and in-plane tension. The studies performed were mainly based on analytical approaches, and the basic relation characterising the behaviour of the plate at the onset of instability was found in an analytical form.

As the result of the general dynamic analysis performed, it was shown that the onset of instability takes place in a divergence (static) form for some critical value of the transport velocity when the frequency of the plate vibrations is equal to zero. It was shown that the flutter modes arise only for higher values of the transport velocity.

Detailed analysis was performed in an analytical manner for static modes of instability. The critical divergence velocity and the corresponding buckling shapes were studied as functions of geometric and mechanical problem pa-

rameters. It was proved that the buckled plate shape is symmetrical, i.e. the antisymmetric shapes correspond to higher values of the transport velocity. It was shown that the meaningful elastic deflections become localised at the vicinity of free edges of the plate, and that the amount of localisation only depends on the Poisson and aspect ratios of the plate.

It is necessary to note that for some buckling problems for plates where the ratio of width to length, b/ℓ, is large, in practice a one-dimensional panel model is used. For this model, the critical parameter is equal to one ($\gamma_* = 1$). However, as was seen from our studies of the two-dimensional buckling problem, the limit of γ_* when the width to length ratio tends to infinity (panel limit) depends on the Poisson ratio, and is less than 1. For any meaningful Poisson ratio ($\nu > 0$), this difference is small but finite. The largest difference is obtained when the Poisson ratio is equal to 0.5. This unusual conclusion is important for rigorous estimation.

Acknowledgement: This research was supported by the MASI Tekes Technology Programme.

References

Archibald, F. R., Emslie, A. G., 1958. The vibration of a string having a uniform motion along its length. ASME Journal of Applied Mechanics 25, 347–348.

Bolotin, V. V., 1963. Nonconservative Problems of the Theory of Elastic Stability. Pergamon Press, New York.

Chonan, S., 1986. Steady state response of an axially moving strip subjected to a stationary lateral load. J. Sound Vib. 107, 155–165.

Frondelius, T., Koivurova, H., Pramila, A., 2006. Interaction of an axially moving band and surrounding fluid by boundary layer theory. J. Fluids Struct. 22 (8), 1047–1056.

Gorman, D. J., 1982. Free Vibration Analysis of Rectangular Plates. Elsevier North Holland, Inc.

Kulachenko, A., Gradin, P., Koivurova, H., 2007. Modelling the dynamical behaviour of a paper web. part ii. Computers & Structures 85, 148–157.

Lighthill, M. J., 1960. Note on the swimming of slender fish. Journal of Fluid Mechanics (9), 305–317.

Lin, C. C., 1997. Stability and vibration characteristics of axially moving plates. Int. J. Solids Structures 34 (24), 3179–3190.

Lin, C. C., Mote, C. D., 1995. Equilibrium displacement and stress distribution in a two-dimensional, axially moving web under transverse loading. ASME Journal of Applied Mechanics 62, 772–779.

Lin, C. C., Mote, C. D., 1996. Eigenvalue solutions predicting the wrinkling of rectangular webs under non-linearly distributed edge loading. Journal of Sound and Vibration 197 (2), 179–189.

Miranker, W. L., 1960. The wave equation in a medium in motion. IBM J. R&D 4, 36–42.
Mote, C. D., 1968. Divergence buckling of an edge-loaded axially moving band. Int. J. Mech. Sci. 10, 281–195.
Mote, C. D., 1972. Dynamic stability of axially moving materials. Shock Vib. Dig. 4 (4), 2–11.
Mote, C. D., 1975. Stability of systems transporting accelerating axially moving materials. ASME Journal of Dynamic Systems, Measurement, and Control, 96–98.
Mote, C. D., Ulsoy, A. G., 1982. Vibration of wide band saw blades. ASME Journal of Engineering for Industry 104, 71–78.
Pramila, A., 1986. Sheet flutter and the interaction between sheet and air. TAPPI-Journal 69 (7), 70–74.
Shin, C., Chung, J., Kim, W., 2005. Dynamic characteristics of the out-of-plane vibration for an axially moving membrane. Journal of Sound and Vibration, 286 (4–5), 1019–1031.
Simpson, A., 1973. Transverse modes and frequencies of beams translating between fixed end supports. J. Mech. Eng. Sci. 15, 159–164.
Swope, R. D., Ames, W. F., 1963. Vibrations of a moving threadline. J. Franklin Inst. 275, 36–55.
Timoshenko, S. P., Woinowsky-Krieger, S., 1959. Theory of plates and shells, 2nd Edition. New York : Tokyo : McGraw-Hill.
Ulsoy, A. G., Mote, C. D., 1980. Analysis of bandsaw vibration. Wood Science 13, 1–10.
Ulsoy, A. G., Mote, C. D., Szymni, R., 1978. Principal developments in band saw vibration and stability research. Holz als Roh- und Werkstoff 36 (7), 273–280.
Wickert, J. A., 1992. Non-linear vibration of a traveling tensioned beam. Int. J. Non-Linear Mechanics 27 (3), 503–517.
Wickert, J. A., Mote, C. D., 1990. Classical vibration analysis of axially moving continua. J. Appl. Mech. 57, 738–744.

Table 1
Values of $\lambda = \gamma_0^2$ for different values of the Poisson ratio ν.

ν	γ_0^2
0.1	0.99997
0.2	0.99939
0.3	0.99621
0.4	0.98533
0.5	0.95711

Table 2
Divergence speed V_0^{div} [m/s] for some example cases, using the physical parameters given in Section 5. In all cases, $2b = 1$ m.

$\nu \setminus \ell$ [m]	10	1	0.1	0.01
0.1	79.0569	79.0570	79.0635	79.7110
0.2	79.0569	79.0570	79.0637	79.7310
0.3	79.0569	79.0570	79.0640	79.7659
0.4	79.0569	79.0570	79.0645	79.8160
0.5	79.0569	79.0570	79.0652	79.8824